Increased Dynamic Range for RFID EM-field Measurements

Santiago Capdevila[1,2], Jordi Romeu[1], Lluís Jofre[1], Jean-Charles Bolomey[3]
[1]Dept- of Signal Theory and Communications, Universitat Politècnica de Catalunya, Barcelona, Spain
[2]Laboratory of Electromagnetics and Acoustics, École Polytecnique Fédérale de Lausanne, Lausanne, Switzerland
[3]Laboratoire des Signaux et Systèmes, Supélec, Gif-sur-Yvette, France

***Abstract*—This paper presents a new methodology to measure the electromagnetic (EM) field using RFID tags, overcoming the limitations in dynamic range arisen by the conventional excitation of RFID tags. The methodology consists in the use of two different signals when interrogating the RFID tag. The first signal is in charge of powering up and triggering the response of the RFID tag, while the second one, with lower power, performs the EM-field measurement. With this approach the dynamic range of the EM-field measurement is increased up to the sensitivity of the receiver, and additionally the non-linearities in the measured field distribution are completely removed.**

I. Introduction

Many industrial, medical or scientific applications rely on the knowledge of an EM field distribution in order to obtain information from a body (e.g. tomographic imaging, non-destructive testing/evaluation, etc.). The Modulated Scatterer Technique (MST) [1], [2] can be efficiently used in order to remotely retrieve the field distribution with a reduced setup complexity, since it does not require any bulky RF connections. However, low-frequency cabling or optical fibers are needed to perform the modulation of PIN diodes [2] or phototransistors [3]. This requirement might be inadequate for some applications, such as sensing of EM-field inside civil engineering structures [4]. Passive Radio Frequency Identification (RFID) tags can constitute an interesting option for these applications, thanks to their capability to modulate the backscattered signal remotely (thus acting like autonomous MST probes), but without any external power supply or low frequency cabling.

Previously, we have shown the feasibility of measuring EM-field distributions [5] using a single low-cost RFID tag or an array of such tags. However, the dynamic range was impaired by the need of a minimum threshold power (P_{th}) to activate the RFID tags.

In this paper, we propose a new approach which allows enhancing the dynamic range when using passive RFID tags to measure an EM-field distribution. According to this approach, the tags are now excited by two signals at different frequencies. One serves to power-on the RFID Integrated Circuit (IC) and the other one to perform the field measurement. Such a dual frequency excitation not only allows significantly improving the dynamic range but, in addition, avoids compensating the non-linearities of the back-scattered response of the RFID tag.

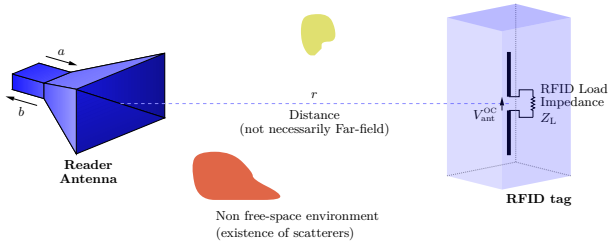

Fig. 1. General RFID sensing scenario, where the RFID tag, embedded in an object, may be located in a far-field and non-free-space conditions

II. RFID EM field measurement

Fig. 1 presents a possible scenario where the electromagnetic field has to be measured somewhere in space, possibly inside of an object. Upon activation by an external interrogating signal transmitted by the reader antenna, the RFID IC responds by alternately changing its impedance between two different values. In fact, with standard passive low-cost RFID tags, the antenna load consists on the RFID IC chip whose input impedance behaves either as an absorbing (Z_{scav}) or reflecting (Z_{SC}) load impedance, and which are switched back and forth according to a sequence to be communicated to the reader. As such, the RFID response at the reader port can be obtained thanks to a reciprocity formulation [6], as a modulated reflection coefficient ($\Delta\rho_{\text{rdr}}$) such that:

$$\Delta\rho_{\text{rdr}} = \frac{\left(V^{\text{OC}}\right)^2}{8P_a R_{\text{ant}}}\left(\tilde{\rho}_{\text{L}_A} - \tilde{\rho}_{\text{L}_B}\right) = \frac{\left(V^{\text{OC}}\right)^2}{8P_a R_{\text{ant}}}\Delta\tilde{\rho}_{\text{L}} \qquad (1)$$

where $\tilde{\rho}_{\text{L}}$ is the complex reflection coefficient of the load [7], [8], R_{ant} is the real part of the input impedance (Z_{ant}) of the tag, P_a is the power transmitted by the reader, and V^{OC} is the open circuit voltage at the antenna port, which is directly related to the field distribution to be measured. As such, it can be seen that the field distribution in a region can be retrieved from the response of a scanning RFID tag, or an array of fixed RFID tags located in this area.

It must be noted that the signal received by the reader, $\Delta\rho_{\text{rdr}}$, is proportional to $\Delta\tilde{\rho}_{\text{L}}$. Consequently, for the measured signal being truly proportional to the field distribution, $\Delta\tilde{\rho}_{\text{L}}$ must remain constant and power independent. It can be easily shown that $\Delta\tilde{\rho}_{\text{L}}$ directly depends on the values of the load impedances

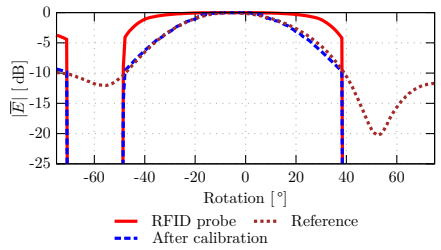

(a) Magnitude

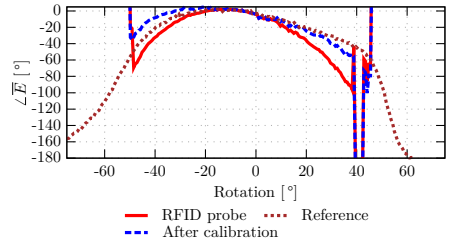

(b) Phase

Fig. 2. Measured radiation pattern with a conventional RFID field probe at 1 GHz. Non-linearities compensated thanks to power-based calibration [5], however the dynamic range is limited by P_{th}, and the radiation pattern can only be measured on a reduced angular range.

(Z_{scav} and Z_{SC}) of the tag antenna:

$$\Delta\tilde{\rho}_{\mathrm{L}} = 2R_{\mathrm{ant}}\frac{Z_{\mathrm{scav}} - Z_{\mathrm{SC}}}{(Z_{\mathrm{scav}} + Z_{\mathrm{ant}})(Z_{\mathrm{SC}} + Z_{\mathrm{ant}})} \tag{2}$$

However, the RFID IC has an input scavenging stage, with a rectifier, to extract the required power to operate from the incident wave. As a direct consequence, both load impedances (Z_{scav} and Z_{SC}) of the RFID tag antenna present a non-linear behavior, and their values directly depend on the power delivered to the IC. As such $\Delta\tilde{\rho}_{\mathrm{L}}$ is not constant during the measurement of the field distribution, because it changes with the power associated to the incident field to be measured. This effect can be clearly seen in Fig. 2 where the field radiated by a horn antenna at 1 GHz is measured by an RFID tag (ALN-9540 [9]) on a 1.5m radius circle. If the tag response was linear, it should reproduce the expected field distribution. However, due to its non-linear behavior, resulting from the power dependence of $\Delta\tilde{\rho}_{\mathrm{L}}$, the measurement presents a distortion. This distortion can be compensated [5] by a proper power-based calibration of the measured response of the RFID tag. As compared to reference results obtained with a small dipole probe, a good agreement can be observed only from $-50\,°$ to $40\,°$, with RFID probe calibrated results. Indeed, outside of this angular range, the incident power reaching the RFID tag is strongly attenuated and is not sufficient to activate the IC. Consequently, the RFID tag remains silent, and the field can no longer be measured. Thus, although conventional RFID tags can be calibrated to correctly retrieve magnitude and phase information of the incident field distribution, the dynamic range is limited by the scavenging circuit. In the previous experiment, the limiting factors are the IC power threshold P_{th}, the power transmitted by the reader P_a, and the attenuation imposed by the scenario, which in this case

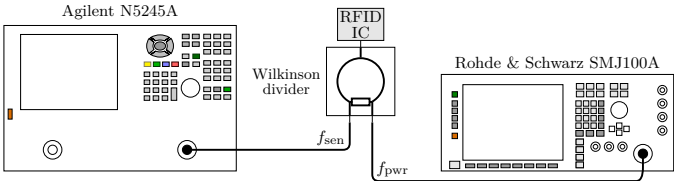

Fig. 3. Experimental setup for the measurement of the input impedance of the RFID IC for an incoming signal composed of two frequencies; a vector signal generator operating at f_{pwr} generates the feeding RFID signal which is combined with a second signal generated by a network analyzer operating at f_{sen}. The calibration of the reference plane is performed using a TRL calibration kit.

depends on the gain of the reader antenna, and the distance between reader and tag.

III. RFID DUAL-FREQUENCY EXCITATION

From the previous section, it results that the dynamic range limitation is strongly dependent on the scenario and the specific conditions of the measurement. Hence, the idea comes that, in order to improve the field sensing capabilities of RFID tags, the powering and the sensing functionalities must be separated. Such a separation can be achieved by using two signals at different frequencies. A first signal — the *powering* signal — at frequency f_{pwr} will serve to power-on the RFID tag and to carry the information that the reader needs to transmit to activate the tag. A second signal — the *sensing* signal — at frequency f_{sen} creates the field distribution that is being measured. Under the assumption that the power delivered to the tag by the first signal is always above P_{th}, the RFID tag can be externally triggered through this signal, in such a way that the modulation of the load impedance of the tag antenna is achieved. Moreover, this modulation will affect any signal, at any frequency, incident on the RFID tag, and in particular the *sensing* signal. Consequently, regardless of the power carried by the *sensing* signal at f_{sen} and even if it is significantly lower than P_{th}, the incident wave to be measured will be modulated and reflected back to the reader according to (1), thus ensuring an enlarged dynamic range.

An additional advantage of the dual-frequency illumination scheme is that, under certain conditions, the non-linearities of the IC impedance ($Z_{\mathrm{scav}} and Z_{\mathrm{SC}}$) at f_{sen} are almost completely removed, thus not requiring any calibration of the measurement. Indeed, provided that the power of the *powering* signal is much larger than that of the sensing signal, the former will fix the operating point of the rectifier and, hence, the input impedance of the rectifying circuit. As a result, the *sensing* signal which is supposed to be much smaller than the *powering* signal, will "see" a set of load impedances (Z_{scav} and Z_{SC}) which is ideally independent of the *sensing* power level P_{sen}.

IV. EXPERIMENTAL CHARACTERIZATION

A. RFID IC input impedance

Before experimentally validating this dual-frequency approach for field measurements, a characterization of the input impedances of an Alien Higgs 2 RFID IC [10] using a

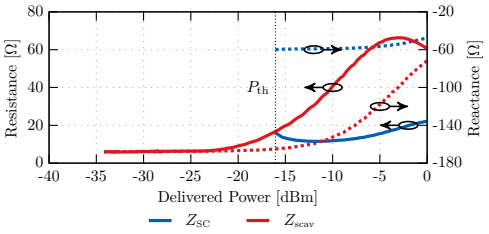

(a) Impedance at $f = 868\,\text{MHz}$ using a single frequency characterization

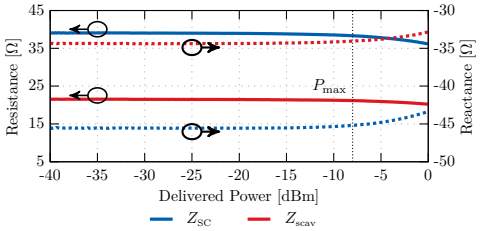

(b) Impedance at $f_{\text{sen}} = 868\,\text{MHz}$ using a dual frequency scheme ($f_{\text{pwr}} = 1\,\text{GHz}$

Fig. 4. Comparison of the RFID IC impedance using (a) a signal consisting of a single frequency at 868 MHz or using (b) two different frequencies, the first one at 1 GHz for activation and the second one at 868 MHz for the impedance measurement.

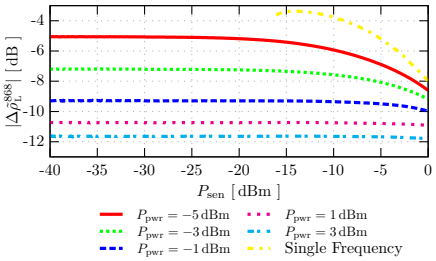

(a) Magnitude

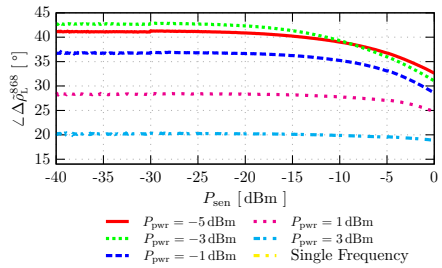

(b) Phase

Fig. 5. $\Delta\tilde{\rho}_{\text{L}}^{\text{sen}}$ at $f_{\text{sen}} = 868\,\text{MHz}$ for a feeding frequency $f_{\text{pwr}} = 1\,\text{GHz}$ for different power levels (P_{pwr}). For every P_{pwr} the response $\Delta\tilde{\rho}_{\text{L}}$ of the RFID IC at f_{sen} remains constant until P_{sen} becomes comparable to P_{pwr}. The last curve presents $\Delta\tilde{\rho}_{\text{L}}$ for a conventional single frequency scheme.

single frequency signal and dual-frequency signals is done. The experimental setup is similar to that used in [11], [12], although for the dual-frequency signal the RFID signal is generated by a vector signal generator at f_{pwr} and combined with a signal at f_{sen} generated by a network analyzer (see Fig. 3). For both setups, a thru-reflect-line (TRL) calibration of the network analyzer establishes the reference plane of the impedance at the RFID IC pads location.

Fig. 4a presents the impedances Z_{scav} and Z_{SC} at 868 MHz for the conventional excitation of the RFID IC: a single frequency is used to activate and measure the RFID response, thus acting simultaneously as *powering* and *sensing* signals. It can be seen that only when the power transmitted by the RFID is above a certain value ($P_{\text{th}} = -16\,\text{dBm}$) the RFID starts responding and both impedances can be measured, whereas only Z_{scav} can be measured below P_{th}. This establishes the lower limit of the dynamic range of this RFID sensor. Moreover, above P_{th} both impedances present a non-linear behavior with respect to the incident power on the IC.

Similarly, Fig. 4b presents the input impedance of the RFID IC using dual-frequency signals: the first one generated by the vector signal generator at $f_{\text{pwr}} = 1\,\text{GHz}$ with a constant transmitted power $P_{\text{pwr}} = 3\,\text{dBm}$ and the second one at $f_{\text{sen}} = 868\,\text{MHz}$ which is power swept by the network analyzer (see Fig. 3). It can be seen that neither impedance has a lower bound like in Fig. 4a. Moreover, it is worth noting that their values remain almost constant until P_{sen} becomes comparable to P_{pwr}, at which point the impedance starts to show a non-linear behavior.

Moreover, as previously mentioned, the *powering* signal establishes the biasing/operating point of the rectifier and thus modifies the value of the RFID IC impedance viewed by the *sensing* signal. Indeed, this is seen in Fig. 5 where the dependence of $\Delta\tilde{\rho}_{\text{L}}$ with respect to P_{sen} is plotted for different values of P_{pwr} covering a range from $-5\,\text{dBm}$ to $+3\,\text{dBm}$. The different curves do not overlap each other, clearly indicating that P_{pwr} is modifying the impedances seen by the *sensing* signal. However, each curve presents a similar behavior consisting of a flat response (in both magnitude and phase) for low values of P_{sen} until a point where non-linearities start to appear on $\Delta\tilde{\rho}_{\text{L}}$, defining an upper bound for P_{sen} linear response.

It is interesting to note at this point that this upper bound ($P_{\text{sen}}^{\text{max}}$) is not constant for every P_{pwr}, but depends on its value. Table I gives the upper bounds $P_{\text{sen}}^{\text{max}}$, defined as the maximum power producing a variation in $\Delta\tilde{\rho}_{\text{L}} \leq 0.1\,\text{dB}$, for each of the curves of the figure. Two opposing trends can be observed in the table. On the one hand, $\Delta\tilde{\rho}_{\text{L}}$ decreases from -5 dB to almost -12 dB when P_{pwr} increases. This directly implies that if P_{sen} is fixed, an increase of P_{pwr} will produce a reduction in the available SNR of the measurement. On the other hand, the upper bound $P_{\text{sen}}^{\text{max}}$ increases from -22 dBm to -1 dBm when P_{pwr} increases. This same behavior can be seen in battery assisted MST probes based on Schottky diodes, whose linearity increases when the local oscillator power increases [13]. As a consequence from these two trends, and taking into account that the variation of $P_{\text{sen}}^{\text{max}}$ is larger than that of $\Delta\tilde{\rho}_{\text{L}}$ if P_{pwr} is increased, it is possible to preserve or even improve the original SNR by increasing P_{sen} in such a way that it compensates the reduction in $\Delta\tilde{\rho}_{\text{L}}$ (while at the same time keeping it in the linear region). This is exemplified in the value of the maximum achievable backscattered power

TABLE I
MAXIMUM P_{sen} FOR A VARIATION OF $\Delta\tilde{\rho}_{\text{L}}$ BELOW 0.1 dB

P_{pwr} [dBm]	$\lvert\Delta\tilde{\rho}_{\text{L}}\rvert$ [dB]	$\angle\Delta\tilde{\rho}_{\text{L}}$ [°]	$P_{\text{sen}}^{\max}$ [dBm]	$\lvert\Delta\tilde{\rho}_{\text{L}}(P_{\text{sen}}^{\max})\rvert$ [dB]	$\angle\Delta\tilde{\rho}_{\text{L}}(P_{\text{sen}}^{\max})$ [°]	$P_{\text{bs}}^{\text{sen}}$ [dBm]
-5.0	-5.0	41.1	-21.8	-5.1	41.0	-26.9
-3.0	-7.2	42.7	-17.1	-7.3	41.8	-24.4
-1.0	-9.3	36.7	-8.2	-9.4	34.7	-17.6
1.0	-10.7	28.3	-2.8	-10.8	26.4	-13.6
3.0	-11.7	20.3	-1.0	-11.8	19.1	-12.8

($P_{\text{bs}}^{\text{sen}} = P_{\text{sen}}^{\max}|\Delta\rho_{\text{rdr}}|^2$) shown in Table I for each P_{pwr}.

B. Dual-frequency field measurement

The characterization of the IC behavior under a dual-frequency signals done in the previous section shows that it is an appropriate approach to use the RFID as a field probe. As such, Fig. 6 presents the experimental setup that is used to evaluate the dual-frequency RFID scheme to measure the field distribution generated by a horn antenna. This experimental setup consists of a bi-static configuration where a vector signal generator operating at $f_{\text{pwr}} = 0.9\,\text{GHz}$ has been positioned at a fixed location and illuminates an RFID tag, with a transmitted power of $P_{\text{pwr}} = 0\,\text{dBm}$. The vector signal generator properly modulates the *powering* signal according to the RFID protocol[14], for triggering a response from the RFID IC attached to the tag antenna. The tag antenna, ALN 9540 [9], consists of a meander line dipole antenna with a length of about 10 cm. A signal generator operating at $f_{\text{sen}} = 1\,\text{GHz}$ is connected to the ridged horn antenna whose pattern is to be measured with a transmitting power $P_{\text{sen}} = -20\,\text{dBm}$. Upon reaching the RFID tag antenna, the *sensing* signal will be scattered and modulated by the variation of its impedance load, according to (1). Finally, a dipole antenna collects the modulated scattered field which is coherently demodulated by a spectrum analyzer, allowing to measure its magnitude and phase.

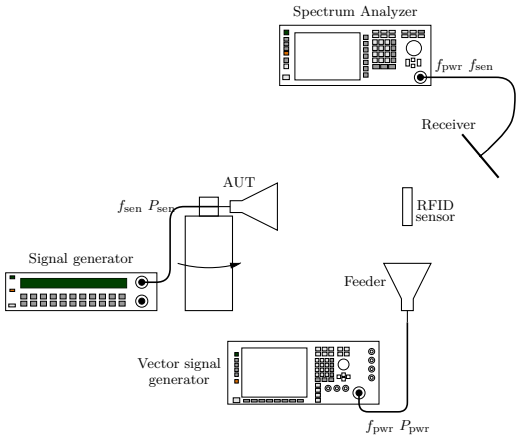

(a) Block diagram

Fig. 6. Experimental setup for the measurement of the radiation pattern of the horn antenna. The horn antenna is placed on top of a rotary stage at 1.5m of the RFID tag in order to measure the radiation pattern at $f_{\text{sen}} = 1\,\text{GHz}$) from $-75\,°$ to $75\,°$.

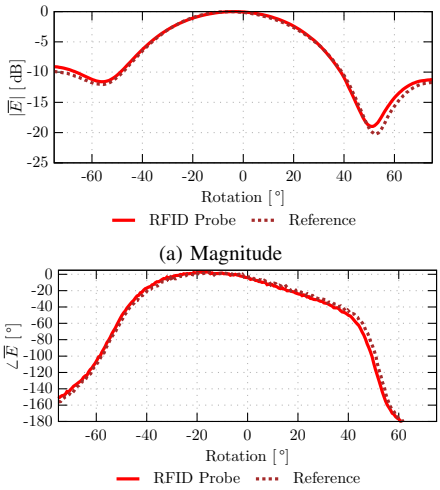

(a) Magnitude

(b) Phase

Fig. 7. Retrieved radiation pattern for the RFID tag operated with a dual-frequency scheme. No post-processing (apart from normalization) is required to recover the expected field distribution.

By simultaneously transmitting both frequencies and rotating the horn antenna from -75 °to 75 °, the amplitude and phase of the field radiated on a 1.5m radius circle can be obtained (see Fig. 7). When comparing these results with those given in Fig. 2, several remarks are worth pointing out. Firstly, the dual-frequency measurement is capable of directly retrieving the field distribution, since as shown in the previous section, the RFID probe response remains fully linear for f_{sen}. Secondly, in Fig. 2 it was shown that the measurement was limited to the angular range from $-50\,°$ to $40\,°$. On the contrary, with the dual-frequency approach the dynamic range is no longer limited by a lower bound and the radiation pattern has been measured over the whole $\pm 75\,°$ angular range, with a very good agreement in both magnitude and phase with the expected field distribution (measured by a small dipole). These results demonstrate that it is possible to accurately measure the low signals at the *sensing* frequency thanks to the presence of the powering signal which is providing the energy required by the RFID tag to operate.

V. SUMMARY AND CONCLUSIONS

This paper has presented the main effects that can be observed when an RFID tag is used as an EM-field probe. Such a probe scavenges the energy from the incident wave and, hence, inherently limits its applicability to EM-field distributions that carry enough power to activate its IC's, thus limiting the dynamic range of measurements. Moreover, even if above the minimum power, non-linear effects affect the measurement and require calibration of the raw data in order to obtain a proper retrieval of the field distribution. As a solution to these problems, this paper has shown how, by using at least two different frequencies, it is possible to simultaneously remove the dynamic range limitations of the measurement while, at the same time, observing a linear response of the

RFID tag for the *sensing* frequency. This approach enhances the dynamic range by removing the power activation threshold from the *sensing* frequency, in such a way that the lower bound will now depend exclusively on the receiver sensitivity. On the other hand, there is an upper bound ($P_{\rm sen}^{\rm max}$) which depends on the measurement scenario and the power of the *powering* signal $P_{\rm pwr}$.

Regarding the SNR of the system, due to the linear behavior at the $f_{\rm sen}$, the behavior of the SNR of the system with $P_{\rm sen}$ is that of a conventional scattering signal. However, it must be noted that the SNR is depending on $P_{\rm pwr}$ in such a way that an increase of $P_{\rm pwr}$ produces a decrease in the SNR of the measurement (through $\Delta\tilde{\rho}_{\rm L}$). Nevertheless, it has been shown that the upper bound $P_{\rm sen}^{\rm max}$ increases more rapidly than $\Delta\tilde{\rho}_{\rm L}$ decreases, so it is still possible to recover, or even improve, the original SNR by increasing $P_{\rm sen}$.

Moreover, in contradistinction with conventional RFID tags, where the powering and sensing signals are both generated by the desired field source, with this dual frequency scheme, the sources of both signals do not need to be radiated by the same and unique antenna. Such a separation between *powering* and *sensing* signals could exploit the architecture of usual bi-static MST probe arrays to develop RFID-based probe arrays for EM-field measurements. Indeed, in such bi-static configurations, the conventional MST collector antenna is designed to illuminate uniformly over the array. Consequently, this antenna could be used to produce a uniform powering signal at the different RFID tags locations, while at the same time it would receive the scattered field modulated by each of the RFID tags.

An application that can directly benefit from this dual-frequency bi-static scheme is EM-field sensing within structures, using embedded sensors, for instance for the assessment of the structural health or water infiltration in civil engineering constructions. In such an application, *wired* MST sensors embedded in the structure are not feasible. On the contrary RFID tags can be embedded into the structure without requiring any external connection, becoming truly wireless and battery-less EM-sensors. Furthermore, thanks to the dual-frequency scheme, the sensing signal can always be kept under the same conditions (position, calibrated output power, etc.) while the independence of the powering signal ensures that the conditions of activation for each of the RFID tags are always fulfilled, regardless of how the changes within the structure affect that signal. Moreover, since the activation threshold $P_{\rm th}$ depends on the RFID IC, it can be used as a reference so that we are always able to keep the *powering* conditions of the RFID IC. If the *powering* conditions are kept constant between measurements, they are comparable overtime and meaningful conclusions on the structure's health can be extracted.

Finally, it is important to note that the dual-frequency scheme can be combined with the multi-load MST concept [15] to improve the sensing capabilities of the RFID tag. Indeed, the dependence of $Z_{\rm scav}(f_{\rm sen})$ and $Z_{\rm SC}(f_{\rm sen})$ with $P_{\rm pwr}$ allows to have different sets of impedance values without making any physical change in the RFID tag, just by changing $P_{\rm pwr}$. As such the RFID response can be measured for different values of $P_{\rm pwr}$ and they can be post-processed using the characterization of the impedance as proposed in [15] to obtain further sensing information on the RFID tag and its environment.

ACKNOWLEDGMENTS

This work was supported in part by the Spanish Interministerial Commission on Science and Technology (CICYT) under projects TEC2010-20841-C04-02 and CONSOLIDER CSD2008-00068

REFERENCES

[1] J. H. Richmond, "A modulated scattering technique for measurement of field distributions," *IRE Transactions on Microwave Theory and Techniques*, vol. 3, no. 4, pp. 13–15, 1955.

[2] J.-C. Bolomey and F. E. Gardiol, *Engineering Applications of the Modulated Scatterer Technique*, A. House, Ed. Artech House, 2001.

[3] H. Memarzadeh-Tehran, J.-J. Laurin, and R. Kashyap, "Optically modulated probe for precision near-field measurements," *IEEE Trans. Instrum. Meas.*, vol. 59, no. 10, pp. 2755–2762, 2010.

[4] K. Donnell and R. Zoughi, "Detection of corrosion in reinforcing steel bars using microwave dual-loaded differential modulated scatterer technique," *IEEE Trans. Instrum. Meas.*, vol. 61, no. 8, pp. 1 –16, aug. 2012.

[5] S. Capdevila, L. Jofre, J. Bolomey, and J. Romeu, "Rfid array probe for em-field measurements," in *Antennas and Propagation Society International Symposium, 2009. APSURSI '09. IEEE*, june 2009, pp. 1 –4.

[6] J. C. Bolomey, S. Capdevila, L. Jofre, and J. Romeu, "Electromagnetic modeling of RFID-modulated scattering mechanism. Application to tag performance evaluation," *Proc. IEEE*, vol. 98, no. 9, pp. 1555–1569, 2010.

[7] K. Kurokawa, "Power waves and the scattering matrix," *IEEE Trans. Microw. Theory Tech.*, vol. 13, no. 2, pp. 194–202, 1965.

[8] P. Nikitin, K. Rao, and R. Martinez, "Differential RCS of RFID tag," *Electronics Letters*, vol. 43, no. 8, pp. 431–432, 12 2007.

[9] *ALN-9540 Squiggle*, Alien Technology. [Online]. Available: http://www.falkensecurenetworks.com/PDFs/DS_ALN_9540_Squiggle_tag.pdf

[10] *Higgs™-2 EPC Class 1 Gen 2 RFID Tag IC. Datasheet*, Alien Tech.

[11] L. Mayer and A. Scholtz, "Sensitivity and impedance measurements on UHF RFID transponder chips," in *International EURASIP Workshop on RFID Technology, Vienna, Austria*, 2007.

[12] S. Capdevila, L. Jofre, J. Romeu, and J. C. Bolomey, "Efficient parametric characterization of the dynamic performance of an RFID IC," *IEEE Microw. Wireless Compon. Lett.*, vol. 22, no. 8, pp. 436–438, 2012.

[13] Q. Chen, K. Sawaya, T. Habu, and R. Hasumi, "Simultaneous electromagnetic measurement using a parallel modulated probe array," *IEEE Trans. Electromagn. Compat.*, vol. 49, no. 2, pp. 263–269, 2007. [Online]. Available: http://ieeexplore.ieee.org/stamp/stamp.jsp?arnumber=4244616

[14] EPCGlobal, *EPC Radio-Frequency Identity Protocols Class-1 Generation-2 UHF RFID Protocol for Communications at 860 MHz – 960 MHz*, January 2005.

[15] S. Capdevila, L. Jofre, J. Romeu, and J. Bolomey, "Multi-loaded modulated scatterer technique for sensing applications," *IEEE Trans. Instrum. Meas.*, vol. 62, no. 4, pp. 794–805, 2013.